Journal of Sound and Vibration (2002) **250**(3), 485–501
doi:10.1006/jsvi.2001.3924, available online at http://www.idealibrary.com on IDEAL®

ACTIVE IMPACT CONTROL SYSTEM DESIGN WITH A HYDRAULIC DAMPER

D. H. KIM

Department of Mechanical Design, Seoul National University of Technology, 172 *Gongneung-dong, Nowon-gu, Seoul* 139-743, *South Korea. E-mail: dhkim@plaza*1.*snut.ac.kr*

J. W. PARK

Department of Mechanical Design & Production Engineering, Graduate School, Seoul National University, San 56-1, *Sinlim-dong, Kwanak-gu, Seoul* 151-742, *South Korea*

G. S. LEE

Agency for Defense Development, Juan Industrial Complex 650, *Juan* 5-*dong, Nan-gu, Incheon-si, South Korea*

AND

K. I. LEE

School of Mechanical and Aerospace Engineering, Seoul National University, Seoul, South Korea. E-mail: lki@plaza.snu.ac.kr

(*Received* 9 *November* 2000, *and in final form* 10 *July* 2001)

We propose a new active impact control (or absorber) system that is able to respond to a highly rapid impact and a large flow rate. The system has advantage over a passive system regarding a feasible pressure and displacement regulation. The impact control system constructs both internal and external dampers, that is its orifice is placed inside and outside the hydraulic cylinder. The designed system has a set of logic valves, which respond rapidly to an external impact and are capable of discharging an instant excessive hydraulic flow, and a servo valve to control the pilot chamber of the logic valve. The impact control system is designed and fabricated based on an appropriate mathematical modelling and its dynamic analysis, and on various control performances. The control performance is verified by simulations and experiments.

1. INTRODUCTION

An impact control or reduction system is designed to respond to an impact force exerted on cylinder chamber. The design objective in this article is how to attenuate the high peak load within an extremely short time (5–20 ms) by carrying out large flow rate over 1000 l/min within that time. In general, the impact control devices are classified into three types: passive, semi-active and active types. The passive impact absorbing is presented in Figure 1. The principal method of controlling a recoil force in a hydro-spring impact absorbing mechanism is to throttle a fluid through an orifice that has various areas during recoil travel. The flow through the orifice generates a fluid force by pressure difference on the piston. The pressure difference across the orifice multiplied by the piston area represents the

0022-460X/02/080485 + 17 $35.00/0

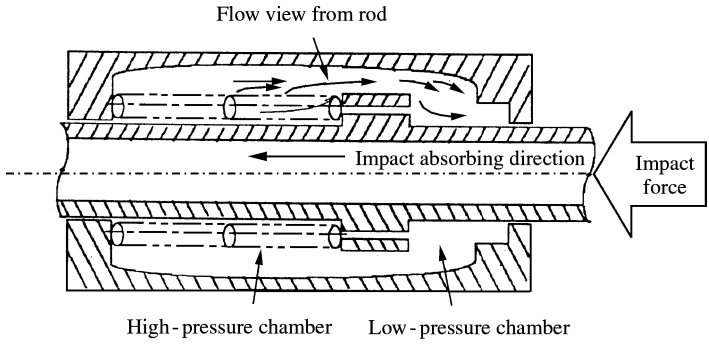

Figure 1. Existing recoil system (passive type).

recoil force acting on the carriage. However, the passive system does not guarantee an optimal performance under various operating conditions because its design objective is only focused on the worst operating condition. The orifice design for a hydraulic impact absorbing mechanism is carried out based on a pre-calculated recoil pressure, hence the controllability for the impact absorber reduces when there exists modelling error or parameter uncertainty. The difficulty in fabricating the orifice is another drawback.

On the contrary, a semi-active type possessing a variable damper shows good performance with a control action, and may maintain its performance under various environments. Many researchers have been working on vibration reduction control using ER (eletrorheological) fluid [1–4] and MR (magnetorheological) fluid [5–7]. These approaches are mainly dedicated to a reduction of vibration using a dramatic change in rheological behavior by applying electrical or magnetic field. For vibration reduction in a vehicle's suspension, a hydraulic damper is utilized. The hydraulic actuator is used in a study on the system's applicability to high-rise buildings [8]. The ER fluid is also applied to a robot actuator [9, 10]. These semi-active types are mainly used for vibration reduction and are adequate to slow external forces. However, under a highly rapid impact, a pressure reduction (or regulation) within a short period is not appropriate for the semi-type damper. As for impact control, minimizing severity of end-stop impact [1] is studied for seat suspension system using ER fluid. Basically, the semi-active control system is dedicated to the control of the one-directional operational system; decreasing the viscosity in ER (or MR) fluid, restricting, or enlarging, the flow rate through orifice without supplying any flow source. This may cause a cavitation in a low-pressure hydraulic chamber for a highly rapid travel.

In this paper, we introduce an impact absorber which is actively adjusting the pressure in the cylinder, and is tackling highly rapid impact and excessive large flow rate. The system adopts logic elements [11, 12] that can discharge a large flow generated in an extremely short period, and a fast-responding servo valve to control the pilot pressure of the logic element. This paper presents a new actively controlled impact system that overcomes the performance limit of the passive and the semi-active impact absorbing system. The system specification is determined by computer simulations and its optimal performance is guaranteed by a suitable selection of logic element and servo valve. A full-scale hydraulic damper capable of providing a pressure reduction up to 40% and piston displacement regulation has been designed and manufactured. We provide a PD-control and a fuzzy control scheme to reduce and regulate the peak pressure generated by the impact force on the piston.

This paper is organized in the following way. Section 2 presents the actively controlled impact system. Section 3 describes a mathematical modelling for the system. Section 4 is

devoted to the detailed explanation of the operating principle and dynamic characteristics of the designed system. Section 5 presents the experimental results by applying the control laws. In section 6, a modified impact control system is addressed. The conclusion is given in section 7.

2. ACTIVE IMPACT CONTROL SYSTEM

2.1. STRUCTURAL DESCRIPTIONS

The designed system consists of a set of logic valves and a servo valve whose components are placed outside the cylinder without changing the passive structure. A hydraulic circuit diagram of this system is shown in Figure 2. Normally, an impact control system adopting only servo valve has the limitation of being applicable to a system with a high peak pressure and a large flow rate for an extremely short duration. To overcome the limitation, a logic valve is adopted. The logic valve is capable of discharging a large flow and regulating a high peak pressure in a short period. As shown in Figure 2, we maintain the passive impact absorbing system and additionally provide two ports outside of the cylinder to install a set of logic valves and servo valve.

The logic valve and the accumulator handle most of the discharging flow rate, whereas the servo valve only controls the pilot flow of the logic valve in the pilot chamber (or a spring chamber) equipped with a restoring spring. The pilot chamber is placed on top of the valve, and the pilot and the main line are designed to be separated from each other in this system. This enables to control both pressure and displacement of the cylinder with only small amounts of power and flow rate. Repeatedly, the servo valve controls the pilot chamber of the logic valve and the logic valve plays a role in discharging or shutting down the large flow rate generated from the cylinder during recoil process. Of course, the inner orifice in the piston is dedicated to discharging most of the total flow rate. As a result of this

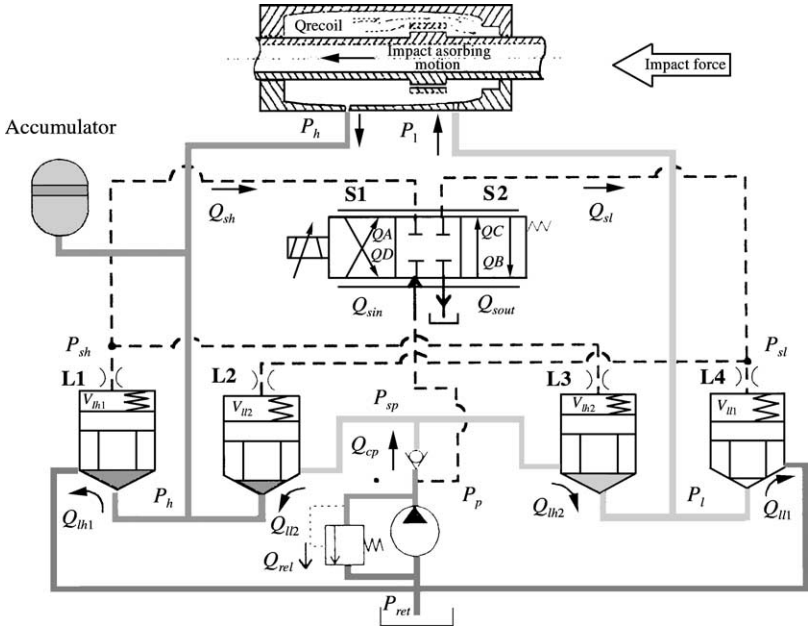

Figure 2. Impact reducing system with active control units.

structure, the instant excessive flow generated by an external impact in a short time can be distributed to the internal orifice and outer orifice which is controlled by logic element and servo valve. On the other hand, the flow in accumulator is used to restore an excessive flow in the recoil process and to supply the flow at the time of the counter recoil motion (return process), hence the speed of the cylinder is increased.

2.2. OPERATING PRINCIPLE

In the recoil motion, the servo valve operates by the command input and moves into the chamber S1. At this stage, the position of servo valve is dependent on the amount of control input as will be shown later in equation (8). The spring chambers of the logic elements L1 and L3 begin unloading when the servo valve is placed anywhere in S1. At the same time, the logic element L3 is then opened by the pump supply pressure, and the fluid flows into the low-pressure chamber of the cylinder. This is an advantage over a semi-active control system since the flow prevents a possible cavitation in the low-pressure chamber. Most of the fluid flows into the low-pressure chamber through the internal orifice and the remaining fluid flows to the logic element L1, where it opens a connection to the tank. On the contrary, the pressure at the pump supply line propagates via the pilot line and the pilot chambers of the logic elements L2 and L4 are loaded. Both elements are therefore held closed, and they isolate the connection from both pump to the cylinder (L2) and the cylinder to the tank (L4). As a result, the high peak pressure during recoil process after impact can be reduced and also controlled by an appropriate control scheme.

In case of the counter recoil motion, the servo valve also operates by the control command and moves into chamber S2. The pump pressure line passes via the pilot line into the pilot chambers of the logic elements L1 and L3, and holds these valves closed. At this stage, the pilot chambers of logic elements L2 and L4 are connected to the tank. The flow from the pump transfers to the high-pressure chamber of the cylinder. The fluid ejected from the low-pressure chamber of the cylinder opens the valve poppet (L4) and thus passes to the tank. In the counter recoil motion, the piston is accelerated by the compressed spring force during the recoil motion, and the supply flow from the pump plays a role in speeding the piston. The piston's position and velocity can be controlled by the servo valve during counter recoil motion.

3. MODELLING OF IMPACT REDUCING SYSTEM

As shown in Figure 2, the designed system consists of various hydraulic components. The main components of the system are a set of logic elements and a servo valve. We present here mathematical models on those components and governing equations of motion. The continuity, cylinder dynamics, and flow equations for calculating pressures and displacements of each component and pipeline are presented. The mathematical model is crucial for an optimal design of the hydraulic components. First, we consider the logic valves (elements).

3.1. LOGIC ELEMENTS

The main characteristic of a logic element is that it is capable of dealing with a large excessive flow rate (up to 3000 l/min) in a short period (less than 20 ms). The logic element here is a type of two-way cartridge valve [11, 12]. With controlling the pressure at the pilot

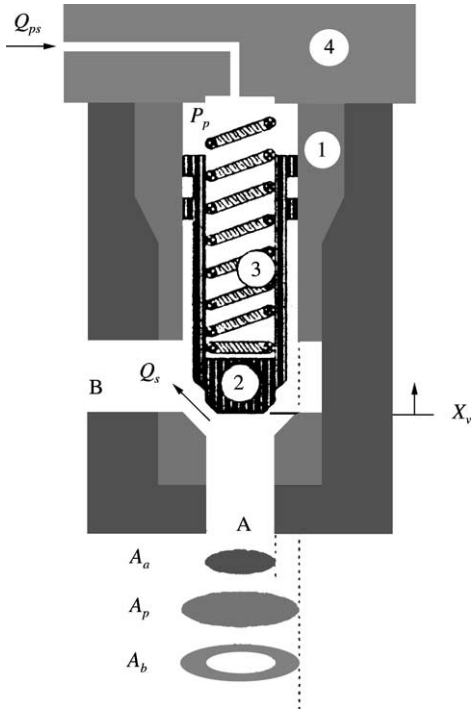

Figure 3. Schematic diagram of logic elements.

chamber by a servo valve, the poppet makes an orifice, hence the chamber pressure in the hydraulic cylinder can be adjusted. As shown in Figure 3, the logic element consists of the cartridge assembly with a bush, the valve poppet, and closing spring together with a control cover. The three areas important for the functioning of the valve are valve seat area (A_a), annulus area at port B(A_b), and area on the spring side (A_p).

Areas A_a and A_b work in an opening direction. Area A_p and the spring play a role in closing the poppet of the valve. The summation of the total resulting force determines whether the logic element opens or closes. When no pressure is applied to the valve, the poppet sits down on the seat.

The opening and the closing forces of the logic element can be written as follows:

$$F_{opening} = P_a A_a + P_b A_b, \tag{1}$$

$$F_{closing} = P_p A_p + F_s, \tag{2}$$

where $F_{opening}$ and $F_{closing}$ represent the opening and closing force of the poppet, respectively, P_a and P_b represent the pressure of ports A and B, P_p denotes the pilot pressure of the logic element and F_s denotes the spring force.

The equation of motion of the valve poppet is represented as follows:

$$m_v \ddot{x}_v = P_a A_a + P_b A_b(x_v) - P_p A_p - F_s - C_v \dot{x}_v, \tag{3}$$

where m_v is the mass of valve poppet, x_v is its displacement, and C_v is the damping coefficient. The flow into the pilot chamber of the logic element (Q_{ps}) can be expressed by

[13]. Next, the pressure derivatives in the high- and low-pressure chambers are written as

$$\dot{P}_{sl} = \frac{\beta}{V_{ll1} + V_{ll2}}(-A_3\dot{x}_{vl1} - A_3\dot{x}_{vl2} + Q_{sl}), \tag{4}$$

$$\dot{P}_{sh} = \frac{\beta}{V_{lh1} + V_{lh2}}(A_3\dot{x}_{xh1} + A_3\dot{x}_{vh2} - Q_{sh}), \tag{5}$$

where $V_{(\cdot)}$ represents the pilot chamber volume of each chamber and β represents the fluid bulk modulus. A_3 is the area of poppet at the pilot chamber, $x_{(\cdot)}$ is the displacement of each logic valve poppet. The flow rates passing the servo valve (Q_{sh}, Q_{sl}) will be written later in equations (9) and (10). The flow rate passing the valve poppet (Q_s) is written as

$$Q_S = C_d A_b(x_v)\text{sign}(P_a - P_b)\sqrt{\frac{2}{\rho}|P_a - P_b|}, \tag{6}$$

where C_d is the flow discharge coefficient and ρ is the fluid density. Here, we see that the orifice area, $A_b(x_v)$, is dependent on the poppet displacement. When the fluid flows through ports A and B, the flow rate is computed based on the geometry between poppet and valve cover. In Figures 4 and 5, the fluid flows through the hatched area and the flow rate changes according to the poppet displacement. The hatched area is written as

$$\begin{aligned} A_b(x_v) &= \pi\left(\frac{r_a}{\cos\theta} + x_v\sin\theta\right)^2\cos\theta - \pi\left(\frac{r_a}{\cos\theta}\right)^2\cos\theta \\ &= \pi(2r_a x_v\sin\theta + x_v^2\sin^2\theta\cos\theta), \end{aligned} \tag{7}$$

where r_a is the radius of the port A and θ is the angle between poppet and valve cover.

3.2. SERVO VALVE

In this study, we adopt the well-known mathematical model of a two-stage servo valve of a mechanical feedback type whose configuration diagram is presented in Figure 6.

The dynamic characteristics of the servo valve spool are modelled by the first order system and are expressed as follows:

$$T_{sv}\dot{x}_{sv} + x_{sv} = K_{sv}i, \tag{8}$$

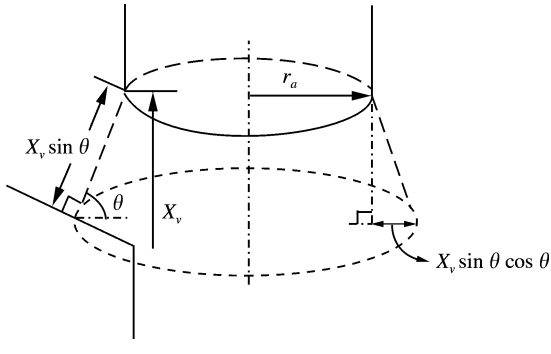

Figure 4. Enlarged view of passing area as poppet moves.

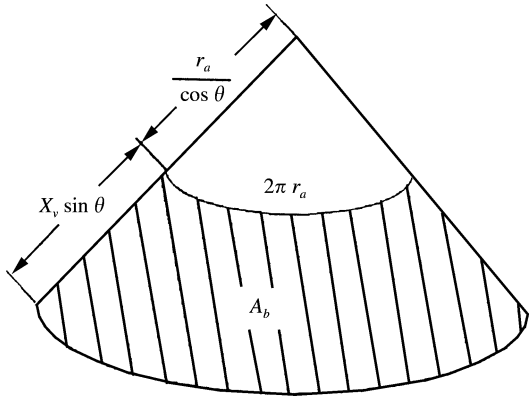

Figure 5. Flow passing area when poppet moves.

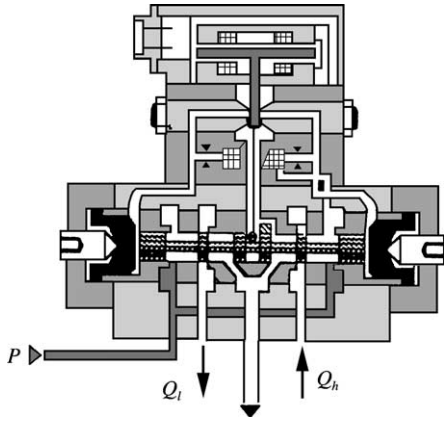

Figure 6. Configuration diagram of servo valve.

where i represents the current in coil, x_{sv} is the servo valve displacement, T_{sv} is the time constant, and K_{sv} is the servo valve gain.

The flow rate equations (Q_{sh}, Q_{sl}) for the servo valve are represented as follows [14]:

$$Q_{sh} = \frac{1}{2} C_d w \sqrt{\frac{2}{\rho}} (1 + \text{sign}(x_{sv})) x_v \sqrt{|P_{sh} - P_0|}, \tag{9}$$

$$Q_{sl} = \frac{1}{2} C_d w \sqrt{\frac{2}{\rho}} (1 + \text{sign}(x_{sv})) x_v \sqrt{|P_{sl} - P_0|}, \tag{10}$$

where P_0 is the pressure of the servo valve's inlet where it is assigned by pump pressure or tank pressure, C_d is again the flow discharge coefficient, and normally has a value of about 0·6–0·7, w is an area gradient on which is dependent the spool diameter (d), and is expressed by πd when the spool diameter is d. The sign (x_{sv}) is a function defined as

$$\text{sign}(x_{sv}) = 1 \quad \text{if} \quad x_{sv} > 0,$$

$$= -1 \quad \text{if} \quad x_{sv} < 0,$$

$$= 0 \quad \text{if} \quad x_{sv} = 0. \tag{11}$$

3.3. EQUATIONS OF MOTION IN CYLINDER

The equation of motion of cylinder can be expressed as follows:

$$m_r \ddot{x}_r = F_i(t) - K(t), \tag{12}$$

where m_r is the total mass of recoil part, x_r is the piston displacement. $F_i(t)$ is the external force by impact, $K(t)$ is the total resistant forces which consist of hydraulic force (F_h), spring force (F_s), and friction force (F_f), which is written as [15]

Here, the hydraulic force is generated by the pressure difference between two chambers. That is

$$F_h = P_h A_h - P_l A_l, \tag{13}$$

where A_h and A_l represent the areas of high- and low-pressure chambers respectively. The spring force is proportional to the piston displacement and the friction force is dependent on the friction coefficient of the packing, where its value is estimated as 0·15 in this system.

The continuity equations for calculating the pressure derivative of each node in the hydraulic circuit of the designed system shown in Figure 2 are as follows. The recoil flow rate between the high- and low-pressure chambers (Q_{re}), and the other flow rates are expressed by the following formulas:

$$Q_{re} = C_d A_{re} \sqrt{\frac{2}{\rho}(P_h - P_l)}, \tag{14}$$

$$\dot{P}_{sp} = \frac{\beta}{V_{sp}}(Q_{cp} - Q_{ll2} - Q_{lh2}), \tag{15}$$

$$\dot{P}h = \frac{\beta}{V_{low}}(-Ah\dot{x}_r - Q_{re} - Q_{lh1} - Q_{ll2}), \tag{16}$$

$$\dot{P}l = \frac{\beta}{V_{low}}(-Al\dot{x}_r - Q_{re} - Q_{ll1} - Q_{lh2}). \tag{17}$$

Here $P_{(\cdot)}$ and $V_{(\cdot)}$ are the pressure and volume of each chamber, respectively, $Q_{(\cdot)}$ is flow through the chamber, and A_h, A_l, are the acting areas of high- and low-pressure chambers. All notations are shown in Figure 2. For simplicity, the detailed descriptions are omitted here. The equations expressed above regarding continuity, flow equation, and actuator dynamics for each component are co-operated to solve the dynamic response, which is shown in detail in the following sections.

4. SIMULATION AND EXPERIMENTAL RESULTS

4.1. SIMULATION RESULTS

In the passive system, the shape of orifice is designed to have an optimal performance under the limited conditions. For the active system, the crucial design factor is how to

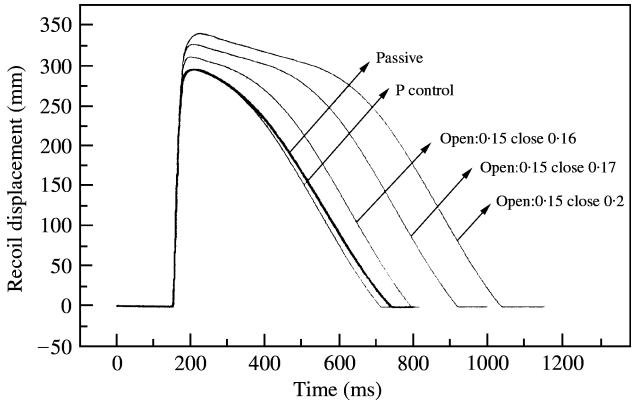

Figure 7. Recoil displacement of the cylinder (simulation).

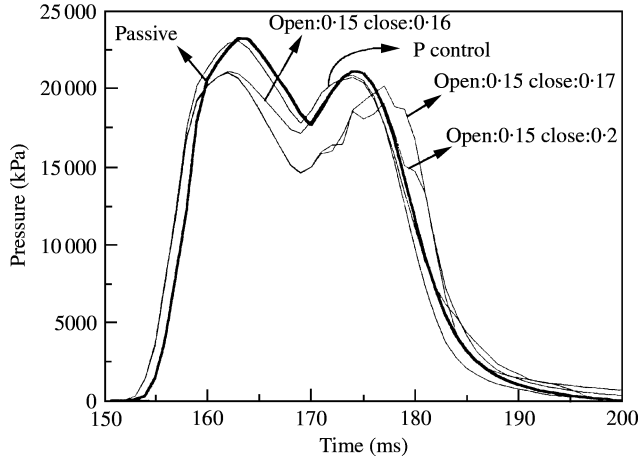

Figure 8. Hydraulic force of the cylinder (simulation).

decide the dimension of logic element. In general, the larger is the size of logic element, the larger is the flow discharge rate, and the slower is the response time. From the mathematical modelling described in the previous section, we first verify a control performance via simulations. Both open loop and feedback system characteristics are analyzed here.

In Figures 7 and 8, "open" means that servo valve is operated in the position S1 and "close" means that the valve operates in the position S2, and the numbers written after open or close denote the valve opening time. As shown in Figure 7 and 8, we see that the more the hydraulic pressure reduces, the longer the displacement of the recoil motion becomes. When the hydraulic force F_h resulting from the pressure difference of the cylinder chamber decreases by the reduced high peak pressure, then the inertia force of recoil mass increases, thus the piston displacement increases. In impact period, the larger logic element size is chosen, the longer cylinder displacement occurs due to the larger discharge rate, hence lower peak pressure is guaranteed. However, too long displacement travel accompanying reduced pressure is not desirable in real. Therefore, a trade-off in choosing the appropriate logic element size is considered by taking into account both the recoil travel and the peak pressure. Based on the simulation results, the size 40 mm in the logic element is

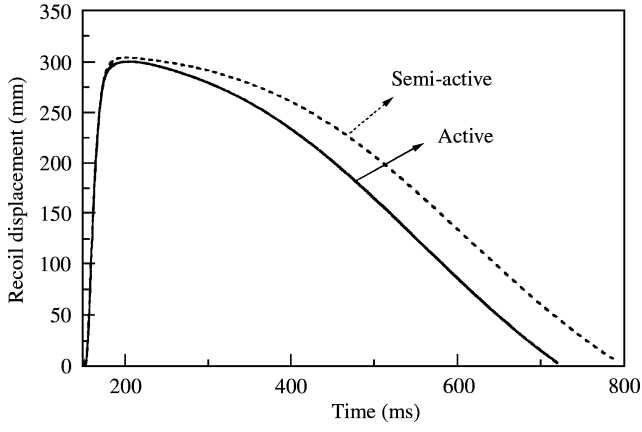

Figure 9. Recoil displacement of the cylinder. (simulation: the comparison of semi-active and active type control).

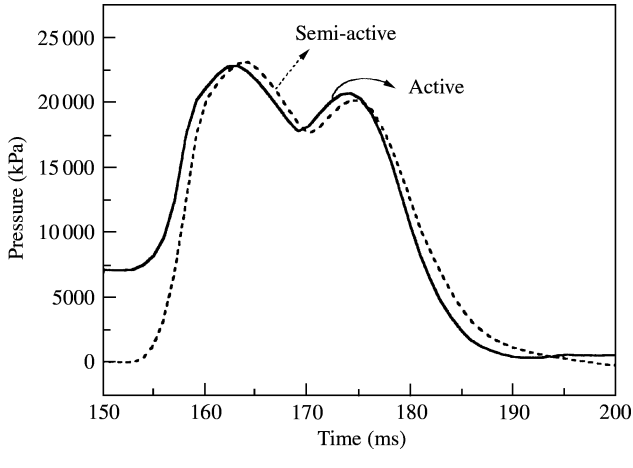

Figure 10. Peak pressure of the cylinder. (simulation: the comparison of semi-active and active type control).

recommended with respect to the short response time and low peak pressure. As shown in Figure 8, the hydraulic force by the pressure difference in the designed system is much lower than that of passive system. Hence, we know that the designed system can control the high peak pressure during the impact by adopting the selected hydraulic components.

In Figures 9 and 10, the control performances are shown between the semi-active control and active control by simulations. The semi-active control system consists of all the components utilized in the active control except the hydraulic power generated by the pump. As seen from the results, the travel distance by the semi-active control is longer than that by the active control. The peak pressure in the chamber by active control is less than that by the semi-active control. Therefore, the active control guarantees better control performance compared to the passive and semi-active control.

4.2. EXPERIMENTAL RESULTS

The performance of the active impact control system is verified experimentally in a setup as shown in Figure 11. Figure 12 shows a schematic diagram for an experimental setup. The

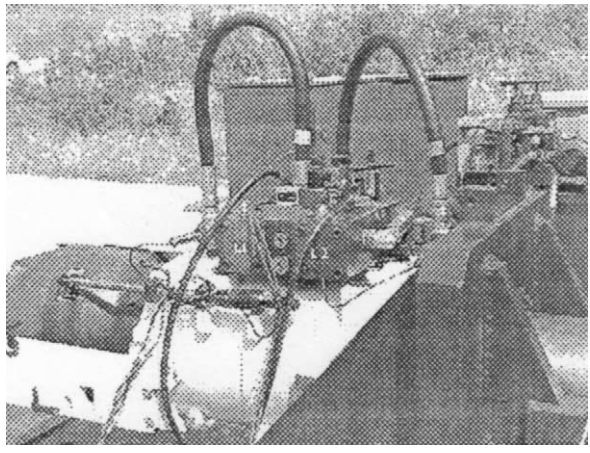

Figure 11. Experimental apparatus for active impulse control system.

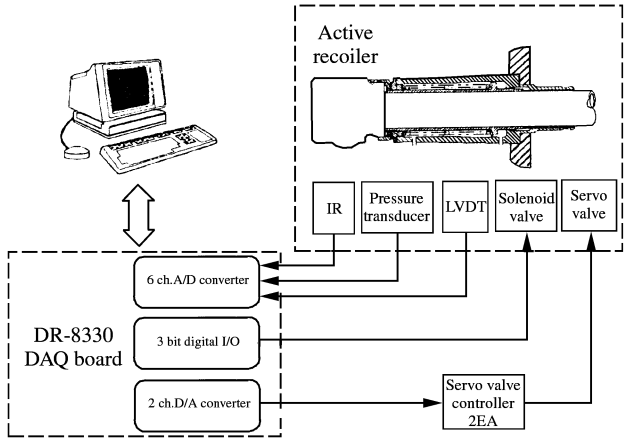

Figure 12. Schematic diagram for the experimental setup.

cylinder is 300 mm in length, and 250 mm in diameter. The impact control system is activated by an external impact, and the pressure and cylinder displacement are measured by a high-bandwidth pressure transducer and a linear variable displacement transducer. (LVDT). The hydraulic parts aiming to control the pressure of cylinder chamber and displacement of the piston are mounted on top of the passive system. Moreover, the complex hydraulic circuit is embedded inside of the manifold, hence the total size of the control system becomes compact.

As described in section 4, we see from Figures 13 and 14 that the low peak pressure gives rise to the displacement increase for the recoil motion. Figure 14 has much coherence with Figure 8 for the passive case; thus, we guarantee that the derived mathematical model is suitable to analyze the dynamic characteristic of the real system. However, the difference between Figures 7 and 13 results from uncertain physical parameters such as bulk modulus, viscosity of fluid, friction, etc.

Since the dynamics of the active impulse control system is complicated due to the non-linearity and parameter uncertainty, a model-based control scheme is not suitable for

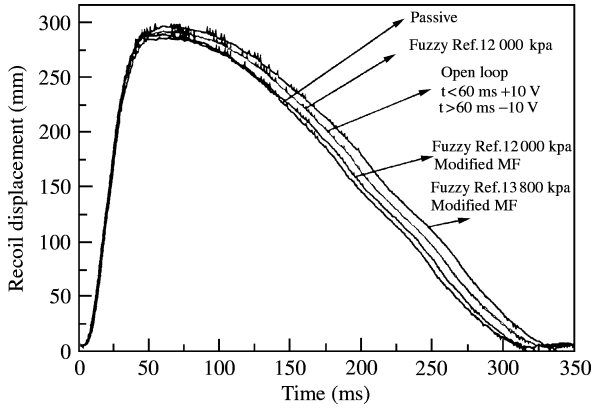

Figure 13. Recoil displacement of the cylinder (experiment).

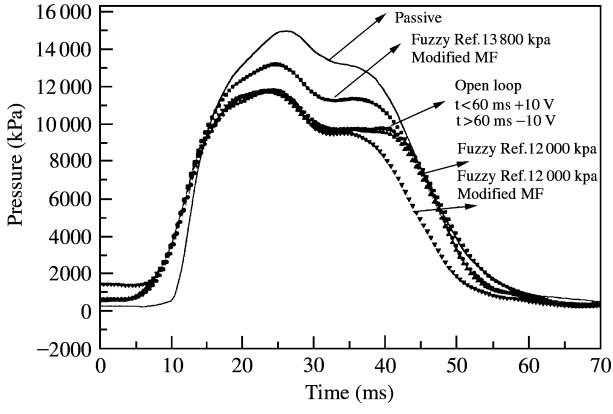

Figure 14. High peak pressure of the cylinder (experiment).

the implementation. Furthermore, a control algorithm with a long computation time is not appropriate for a system requiring an extremely short period of operation. Therefore, we utilize a fuzzy control algorithm to cope with the uncertain parameters and highly rapid response. As shown in Figure 14, the pressure drop by the open loop and the fuzzy control with a reference 12 000 kPa is almost similar. This implies that the designed system could be sufficiently controlled by using a feedback control with highly rapid responding hydraulic components.

A simple control algorithm (open-loop control) and a fuzzy control are applied to the designed system, and the reference pressure is set at 9000 kPa. As a result, the recoil pressure is regulated to the reference range. By the active control system, we could reduce the peak pressure down to 40%. Remarkably, the system guarantees a feasible pressure control under the extremely rapid impact and large flow rate. The pressure is regulated and the piston displacement is shown in Figure 13, where the controlled system takes a longer time to reach the original position after counter recoil process than the passive system. The control surface of the fuzzy controller [16] used in the experiment is presented in Figure 15 and the center values of the membership function for pressure control are presented in Table 1.

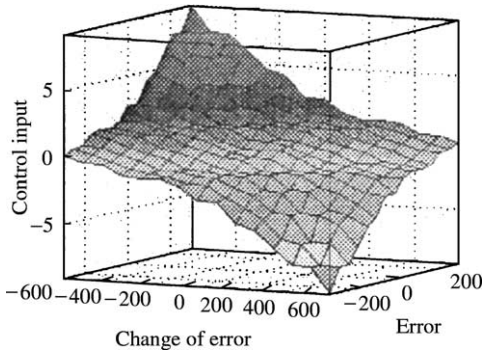

Figure 15. Control surface of the fuzzy controller.

TABLE 1

The center values of fuzzy MF

Membership functions (triangle)	Error (100 kPa)	Change in error (100 kPa)	Control input (V)
NBL	−21	−42	−10·0
NSL	−17·5	−35	−6·95
NBM	−14	−28	−4·45
NSM	−10·5	−21	−2·50
NBS	−7	−14	−1·11
NSS	−3·5	−7	−0·28
ZR	0	0	0
PSS	3·5	7	0·28
PBS	7	14	1·11
PSM	10·5	21	2·50
PBM	14	28	4·45
PSL	17·5	35	6·95

5. MODIFIED SYSTEM

The impact control system presented in the previous section has a drawback somehow because the main flow line is associated with the pilot line whose role is to control the logic valve. This sometimes prevents a precise control because each logic valve may lose its role during the control process. In other words, at recoil motion the logic valves L1 and L3 should be open while logic valves L2 and L4 remain closed. At almost the end of the recoil motion, the main pressure drops down and the pressure is transferred to the pilot line. Then, the pressure is not high enough to keep the logic valves L2 and L4 closed. Therefore, the main line that stems from the main cylinder needs to be separated with a pilot line. The new system contributes to separating the pilot line by placing a gear pump with a small capacity. Here, we present a modified impact control system as shown in Figure 16. For this purpose, two highly rapid solenoid valves are added before the servo valve. The solenoid valves are constructed in order to cope with an emergency state such as electric shut down, by directly discharging large flow to the tank at recoil process. The experimental results obtained by adopting PD and fuzzy control are presented in Figures 17–19, and they show better performance regarding a pressure regulation than the previous system. As shown in Figure 17, the recoiling and returning displacement does not show distinguished performance

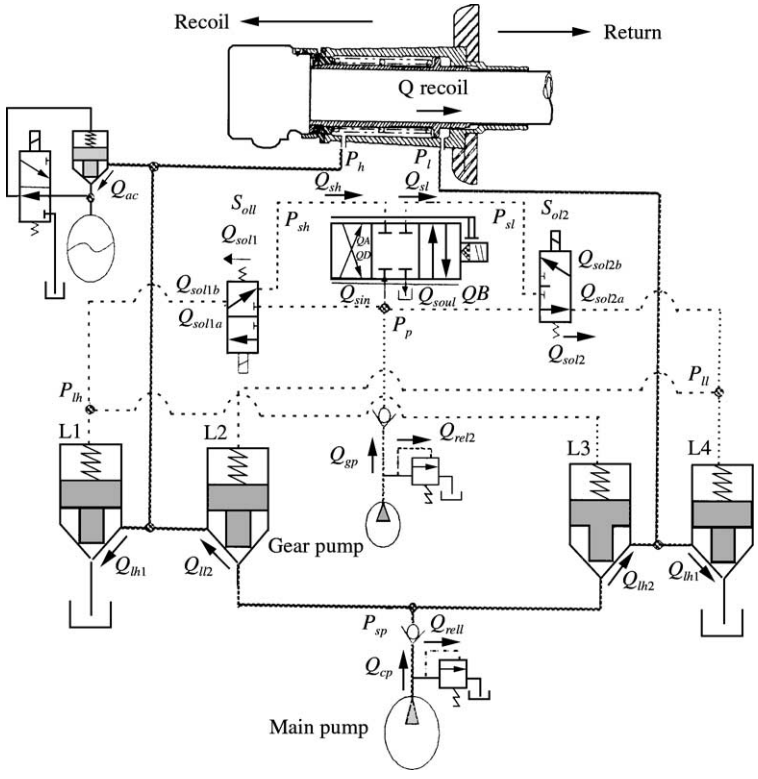

Figure 16. Modified impact control system.

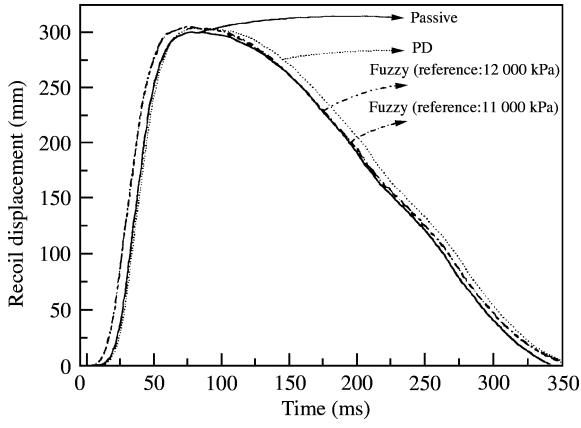

Figure 17. Piston displacement of recoil and return process for the modified system (experiment).

compared to the passive system. However, the high chamber pressure is regulated to track the reference pressure of 16 000 kPa.

In particular, the pilot pressures at L1–L4 are measured (Figure 19) and we see that L1 and L2 do not have distinguished pressure difference at recoil process even if each pilot pressure at each chamber is assigned oppositely. This happens because the flow at the pilot chamber is not sufficiently discharged to the tank in an extremely short period in recoil

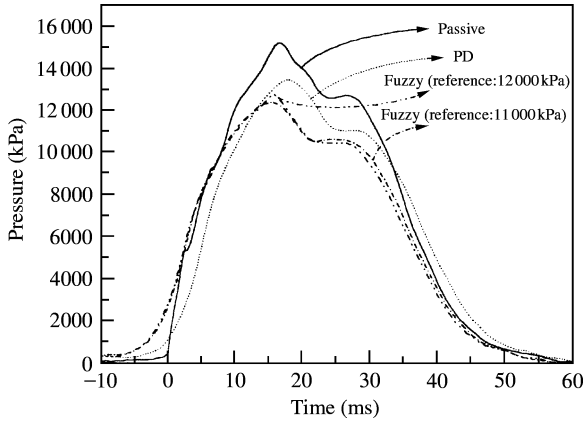

Figure 18. Pressure histories of recoil process for the modified system (experiment).

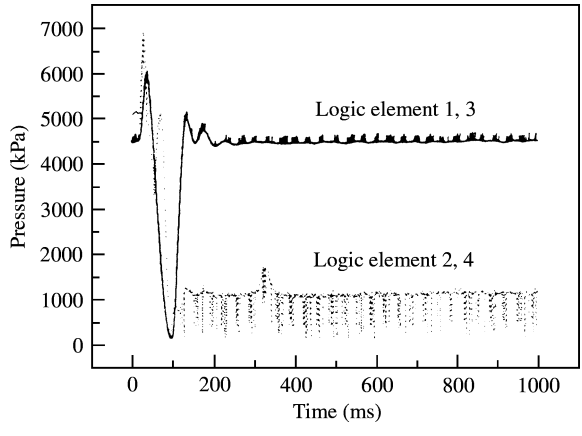

Figure 19. Pilot pressure histories of logic elements for the modified system (experiment).

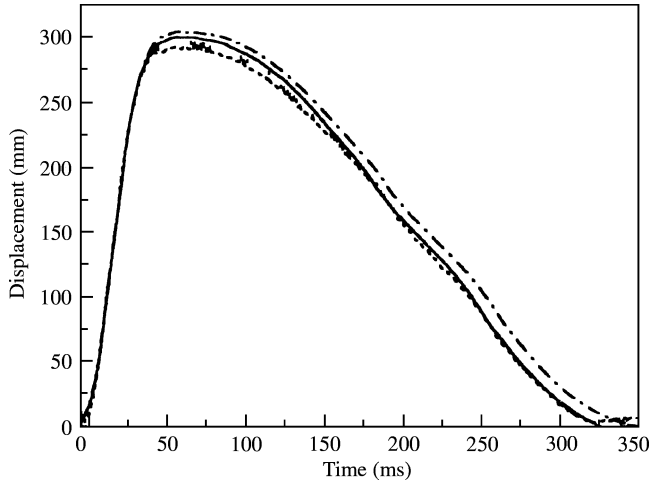

Figure 20. Displacements for the passive, previous, and modified systems (experiment). ——, passive; – · – · –, modified; ·····, old. Reference: 12 000 kPa.

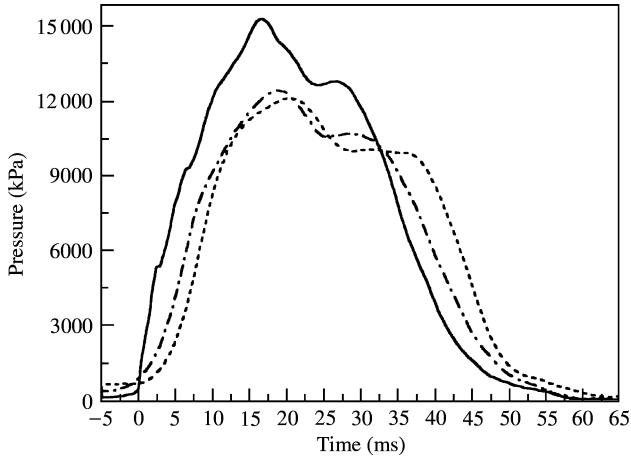

Figure 21. Pressure histories of the passive, previous system, and modified systems (experiment). ——, passive; –·–·–, modified; ·····, old. Reference: 12 000 kPa.

TABLE 2

Control performance for each control scheme

	Passive	PD control	Fuzzy control
Ratio of peak pressure to the reference	1·3	1·15	1·04
Pressure reduction (%)	0	20	40
Relative to the passive			
Travelling displacement (mm)	350	360	360

process. Thus, the pressure increases instead. To reduce the pressure, a larger size of servo valve is needed; however, this causes a slow response. Therefore, a compromise between the pressure reduction and response time is needed in selecting a servo valve. A proper servo valve is chosen by simulations, and the experimental results by this servo valve are shown in Figures 17 and 18. The displacement is not much different compared to the previous model; however, the pressure is tracking better to the reference pressure by adopting fuzzy control algorithm than the previous system. In Figures 20 and 21, the control performance is compared for the previous active system and the modified system. The displacement does not show distinguished difference between the two systems. However, the pressure by the modified system is more reduced than in the previous case. In consequence, this has the effect of decreasing the impact energy. Next, the control performance by the modified system for each control scheme is summarized quantitatively in Table 2.

6. CONCLUSIONS

The active impact control system that overcomes the performance limit of the classical passive system is designed and manufactured. The possibility of regulating the high peak pressure of the system in an extremely short time is verified. The developed system is constituted by a set of logic valves and a servo valve to the system requiring an extremely rapid response and high capability of bypassing an instant excessive flow. For the

appropriate selection of the logic valve and servo valve *in priori*, simulations based on the mathematical modelling are done. After that, experiments have been carried out to verify the performance of the developed system.

In view of these results, we confirm that the hydraulic servo control system can provide a solution for the system requiring a highly rapid response and large flow rate in an extremely short period under an external impact. Thus, the system can be recommended as a good reference. Whereas the system using ER normally controls a vibration by a variable damper, the hydraulic system can control a resulting force exerted on the piston by a hydraulic damping through an internal and external orifice. To guarantee a better performance than that of the system introduced first, a modified impact control system that possesses a separate pilot line with the main hydraulic line is addressed and experiments are then done.

However, further studies remain here, such as the optimization of the system design with respect to how we could distribute the passive system and the active system. A full active control system (excluding the passive part) doe not guarantee the best control performance due to the limitation of the response and large flow discharge in the logic element. Furthermore, an appropriate control algorithm, which accounts for a better performance than the schemes adopted in this paper, needs to be investigated and applied to the system.

REFERENCES

1. X. Wu and M. J. Griffin 1997 *Journal of Sound and Vibration* **203**, 781–793. A semi-active control policy to reduce the occurrence and severity of end-stop impacts in a suspension seat with an electrorheological fluid damper.
2. S. Hidaka, Y. K. Ahn and S. Morishita 1999 *Journal of Vibration and Acoustics* **21**, 373–378. Adaptive vibration control by a variable-damping dynamic absorber using ER fluid.
3. N. H. McClamroch, D. S. Oritz, H. P. Gavin and R. D. Hanson 1994 *Proceedings of the* 33*rd IEEE Conference on Decision and Control*, Lake Buena Vista, FL, Vol. 1, 97–102. Electrorheological dampers and semi-active structural control.
4. D. N. Wu, L. C. Jaw 1998 *Proceedings of the* 1998 *American Control Conference*, Vol. 6, 3425–3429. ER fluid dampers and their application in shock mitigation.
5. J. D. Carlson and B. F. Spencer Jr. 1996 *Third International Conference on Motion and Vibration Control*, *Chiba*, September 1–6, 35–40. Magneto-rheological fluid dampers for semi-active seismic control.
6. B. F. Spencer Jr., J. D. Carlson, M. K. Sain and G. Yang 1997 *Proceedings of the American Control Conference*, Albuquerque, New Mexico, Vol. 1, 458–462. On the current status of magnetorheological dampers: seismic protection of full-scale structures.
7. R. Stanway, 1996 *Actuator Technology*: *IEE Colloquium on Current Practice and New Developments* (*Digest No*: 1996/110). 1–6. The development of force actuators using ER and MR fluid technology.
8. N. Niwa, T. Kobori, M. Takahashi and N. Kurata 1998 *MOVIC*'98, Zurich, Switzerland, Vol. 2, 607–612. Application of semi-active hydraulic damper to an actual building.
9. N. Takesue, G. Zhang, J. Furusho, M. Sakaguchi 1998 *Proceedings of the* 1998 *IEEE International Conference on Robotics and Automation*, Lueven, Belgium, Vol. 3, 2470–2475. Precise position control of robot arms using a homogeneous ER fluid.
10. Y. Kondoh and S. Yokota 1999 *Proceedings of the* 1999 *IEEE/RSJ International Conference on Intelligent Robots and Systems*, Vol. 3, 1757–1761. Movable electrode-type ER actuators (proposal of linear-type and rotary-type METERA).
11. Rexroath-seki *Total Catalog*. Mannesmann Rexroath Ltd.
12. A. Schmitt and R. A. Lang 1989 *Hydraulic Trainer*, *vol.* 4. Logic Element Technology, Mannesmann Rexroath Ltd.
13. J. Watton 1989 *Fluid Power System*. Englewood Cliffs, NJ, Prentice-Hall.
14. H. E. Merritt 1967 *Hydraulic Control Systems*. New York: John Wiley & Sons.
15. Military Handbook 1998 *Recoil Systems*. Department of defense.
16. K. M. Passino and S. Yurkovich 1998 *Fuzzy Control*. Reading, MA, Addison-Wesley.